Directionally electrodeposited gold nanoparticles into honeycomb macropores and their surface-enhanced Raman scattering†

Peiqin Tang and Jingcheng Hao*

Received (in Montpellier, France) 10th March 2010, Accepted 16th March 2010
First published as an Advance Article on the web 1st April 2010
DOI: 10.1039/c0nj00192a

The ordered honeycomb films of dioctadecyldimethylammonium ($DODMA^+$)-encapsulated sandwich-type $[(Mn(H_2O)_3)_2(WO_2)_2(BiW_9O_{33})_2]^{10-}$ ($\{Mn_2Bi_2W_{20}\}^{10-}$) are used as templates to directionally electrodeposit gold nanoparticles into their macropores. Consequently, the prepared hierarchical Au-filled films present a strong surface-enhanced Raman scattering of rhodamine 6G molecules.

Ordered porous films have become an attractive hotspot because of their potential applications in catalysis, separation and micrographic technology. Self-assembly is a useful method to fabricate ordered honeycomb films with hexagonally arranged macropores on solid substrates.[1] Very recently, we have found that nanoscaled polyoxometalates (POMs), after surface-encapsulation by cationic double-chain surfactants, are good hybrids to self-assemble into ordered honeycomb films at an air/water interface through a simple solvent evaporation process.[2,3] POMs are generally soluble in water in the form of giant ions. They can be easily surface-modified by oppositely-charged surfactants or polyelectrolytes, which, furthermore, stabilize POMs. The assembly of POMs with surfactants and polyelectrolytes into LB films, LbL multilayer films and casting films have been gradually investigated.[4–7] However, making use of them is a challenge in POM chemistry. Herein, we have obtained an ordered porous honeycomb film of a surfactant-encapsulated POM. Furthermore, we use it to modify an indium tin oxide (ITO) electrode in order to directionally electrodeposit Au nanoparticles into its macropores. In particular, surface-enhanced Raman scattering (SERS) of organic molecules and the electrochemical properties of the produced hierarchical Au-filled honeycomb films are investigated.

Sandwich-type $Na_6(NH_4)_4[(Mn(H_2O)_3)_2(WO_2)_2(BiW_9O_{33})_2]^{8}$ ($\{Mn_2Bi_2W_{20}\}$) dissolves in water and forms the $\{Mn_2Bi_2W_{20}\}^{10-}$ giant anion. Taking $\{Mn_2Bi_2W_{20}\}^{10-}$ as a typical example, the double-chain cationic surfactant dioctadecyldimethylammonium chloride ($DODMA^+Cl^-$) can electrostatically interact with $\{Mn_2Bi_2W_{20}\}^{10-}$ in the molar ratio of 10 : 1. Finally, hydrophobic $(DODMA)_{10}\{Mn_2Bi_2W_{20}\}$ clusters that can be easily transferred into chloroform are formed. As shown in Scheme 1, a chloroform solution of $(DODMA)_{10}\{Mn_2Bi_2W_{20}\}$ (1.7 mg mL^{-1}) was cast at an air/water interface at room temperature. It initially formed a lens-shape liquid film on the water surface. After complete evaporation, the ordered honeycomb film self-assembled. The thin opaque solid film was directly transferred onto analytical substrates, including ITO-coated glass and monocrystalline silicon. An SEM image of the self-assembled honeycomb film is shown in Fig. 1a, indicating open pores and a monolayer film with hexagonally arranged ordered macropores of average diameter 1.8 μm. The AFM image (Fig. 1b) shows that the honeycomb film possesses a thickness of about 1 μm.

After fabricating the ordered porous honeycomb films, the functionalization of them and/or their templating applications is necessary to find alternatives. As is well known, electrodeposition is an effective method to grow a material, and it has been widely used to synthesize Au,[9] Ag[10] and Cu[11] particles by using porous alumina[12,13] and mesoporous silica[14] templates. It has also proved to be practically useful for functionalizing our newly investigated honeycomb films of surfactant-encapsulated POMs by electrodepositing Au nanoparticles into their macropores.

We next transferred our ordered porous honeycomb film of $(DODMA)_{10}\{Mn_2Bi_2W_{20}\}$ onto conductive indium tin oxide (ITO)-coated glass and used the prepared ITO as a working electrode (WE) to electrodeposit Au nanoparticles by cyclic voltammetry (CV) in a 0.5 mM $HAuCl_4$ and 0.1 M KNO_3 aqueous solution (pH = 6.14). In order to induce the complete deposition into honeycomb film macropores, the bare region of the working electrode was insulated by carefully covering it with nail polish. Fig. 1c shows that Au nanoparticles were

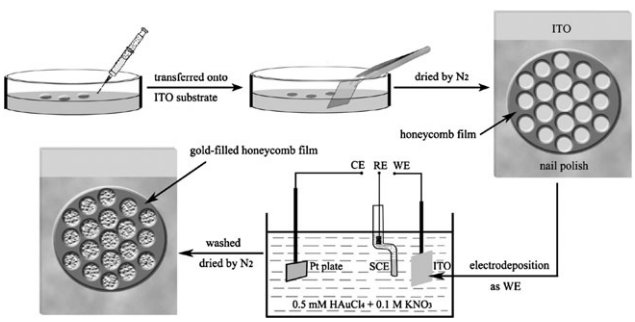

Scheme 1 The experimental procedure from the fabrication of the honeycomb film at an air/water interface to the electrodeposition of Au nanoparticles into the honeycomb macropores.

Key Laboratory of Colloid and Interface Chemistry, Shandong University, Ministry of Education, Jinan 250100, P. R. China. E-mail: jhao@sdu.edu.cn; Fax: +86 531-88564464; Tel: +86 531-88366074

† Electronic supplementary information (ESI) available: Chemicals and other experimental procedures. SEM images of gold nanoparticles, which were electrodeposited onto bare ITO-coated glass without the honeycomb film template.

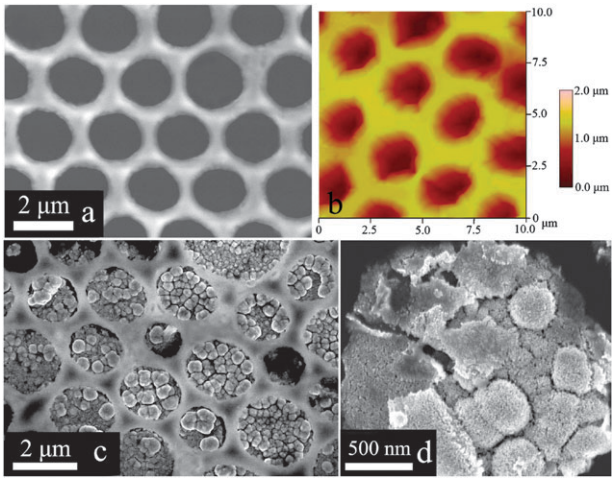

Fig. 1 (a) SEM and (b) AFM images of the self-assembled honeycomb films of $(DODMA)_{10}\{Mn_2Bi_2W_{20}\}$ at an air/water interface. (c) SEM image of the hierarchical array with Au nanoparticles directionally electrodeposited into the honeycomb macropores. (d) A high magnification SEM view of Au nanoparticles in one pore after removing the honeycomb film template by chloroform dissolution.

well-deposited into the honeycomb pores but not on the walls. This is very reasonable according to the formation mechanism of honeycomb films.[3] During the self-assembly, because of the rapid evaporation of chloroform, many micrometer water droplets are condensed and act as templates for pores. Meanwhile, $(DODMA)_{10}\{Mn_2Bi_2W_{20}\}$ clusters are deposited on the walls. After transferring the honeycomb films onto ITO-coated glass, the macropores are open to the ITO conductive surface, which can provide channels for electron transfer onto the working electrode. However, $(DODMA)_{10}\{Mn_2Bi_2W_{20}\}$ clusters are highly hydrophobic, and the carbon chains of DODMA are insulative. Thus, electronic conduction on the walls is prevented. Consequently, Au nanoparticles prefer to electrodeposit into the macropores rather than deposit on the walls. Finally, a hierarchical Au-filled honeycomb film of surfactant-encapsulated POMs is obtained. As obviously observed from Fig. 1d, in which the honeycomb film template was removed by chloroform dissolution, very small Au nanoparticles tend to grow gradually into larger aggregates of hundreds nanometers.

The electrodeposition of metal particles is a delicate process, and the growth mechanism of nanoparticles within templates remains speculative.[15] We therefore speculate that, since the honeycomb film template has ordered pores of nearly uniform size, the Au-deposited honeycomb films can be considered as a porous electrode. It has been proved that the electrochemical process could be diffusion-limited within porous electrodes.[16] Therefore, it can be inferred that the diffusion rate should play an important role during the electrodeposition. The diffusion rate of ions in small pores is slower than in large pores, and the cathode current densities through small pores are smaller. Therefore, it is difficult to fluently carry out the electrodeposition of Au nanoparticles into small pores under our experimental conditions. As shown in Fig. 1c, the few small pores of $\sim$1 μm diameter are hardly filled during the electrodeposition. However, in larger pores, new nuclei are easily formed, thus many and large Au nanoparticles fill them.

Under the same conditions, the electrodeposition was also carried out on bare ITO-coated glass without the honeycomb film template. The morphologies of the electrodeposited Au nanoparticles are shown in Fig. S1 (see the ESI†). Besides the small ($\sim$30 nm) Au nanoparticles non-selectively close-packed onto the ITO surface, larger Au nanoparticles of hundreds nanometers are also randomly present. Comparing the Au nanoparticles electrodeposited without the honeycomb film template and the ones with the honeycomb film template, Au nanoparticles can be controlled to selectively and territorially grow by honeycomb film templates.

Some noble metal (Au and Ag) nanoparticles have been investigated to enhance the Raman scattering signal of organic molecules.[17,18] Rhodamine 6G (R6G) is a strongly fluorescent xanthene derivative. When it is excited into its visible absorption band, R6G can show a molecular resonance Raman effect. According to a reported method,[19] we prepared samples for Raman measurements by drop casting 5.0 μL of a 3.7×10^{-6} mol L^{-1} R6G/methanol solution onto heated (116 °C) analytical substrates, including bare ITO-coated glass (sample A), honeycomb film-covered ITO-coated glass (sample B), Au-deposited ITO-coated glass, on which Au nanoparticles were electrodeposited without the honeycomb film template (sample C), and with the honeycomb film template (sample D; the template was dissolved in chloroform before Raman preparation). After the rapid evaporation of methanol, the uniform films of R6G were added to analytical substrates. Raman measurements were carried out by laser confocal Raman microspectroscopy (LabRAM HR800, HORIBA Jobin Yvon, France) with excitation at 532 nm and 50 mW. All spectra were accumulated over 20 s. As shown in Fig. 2, except for the two broad peaks at 570 and 1100 cm^{-1}, which are assigned to the vibrations of the glass, no Raman signal for R6G was detected for sample A (curve a). R6G was not detected for sample B (curve b), and because of the coverage of the honeycomb film, it was also difficult to observe the glass vibrations. Interestingly, R6G signals were obviously detected for sample C (curve c) and sample D (curve d). It is inferred that the electrodeposited Au nanoparticles in samples C and D possess surface-enhanced Raman scattering (SERS) of R6G molecules. In particular, sample D presents a much stronger SERS effect, which maybe due to the hierarchical structure of the microscaled array and nanoscaled particles. The results indicate that the hierarchical Au-filled honeycomb film is a good detector of R6G molecules. The Raman shifts at 612 and 773 cm^{-1} are assigned to the C–C–C ring in-plane bending vibration and the C–H out-of-plane bending vibration of the xanthene skeleton, respectively. The bands at 1090, 1125 and 1183 cm^{-1} are assigned to C–H in-plane bending vibrations. The C–O–C stretching vibration occurs at 1276 cm^{-1}. The bands at 1309, 1361, 1420, 1504, 1531, 1573, 1600 and 1649 cm^{-1} are assigned to the aromatic C–C stretching vibrations.[20]

The electrodeposited Au nanoparticles are also suitable for the subsequent metallization of honeycomb films of surfactant-encapsulated POMs and the fabrication of particle-type films with interesting electrical properties. The honeycomb film of

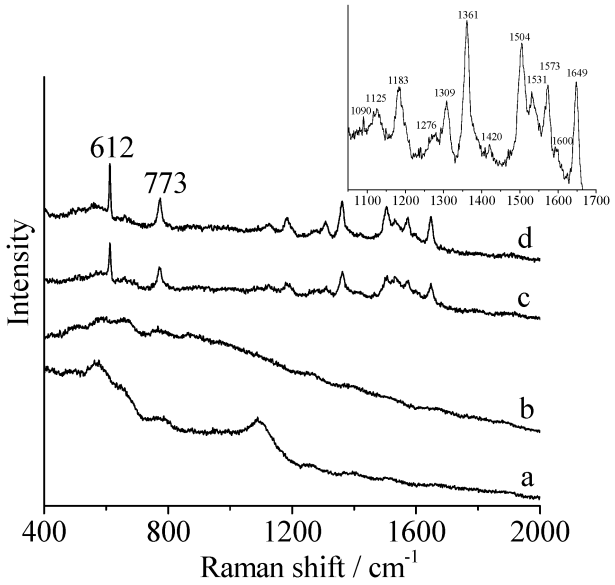

Fig. 2 Raman scattering spectra of R6G on (a) the bare ITO-coated glass, (b) the honeycomb film-covered ITO-coated glass and (c, d) the Au-deposited ITO-coated glass. The Au nanoparticles were electrodeposited without the honeycomb film template in (c) and with the honeycomb film template in (d). The honeycomb film template was dissolved in chloroform before Raman preparation for sample D. The inset shows the magnification of curve d from 1050 to 1700 cm^{-1}. The Raman measurements were all conducted using an excitation wavelength of 532 nm and with a 20 s accumulation.

$(DODMA)_{10}\{Mn_2Bi_2W_{20}\}$ was hardly electrochemically active in a 0.1 M KNO_3 aqueous solution from −0.6 to 1.4 V. However, the rich electrochemical properties of the extended Au-filled honeycomb film were detected through cyclic voltammetry (CV) at different scan rates (Fig. 3a). Two couples were observed with oxidations at 1.14 and 0.27 V *vs.* a saturated calomel electrode (SCE). It was also found that the redox peak current linearly scales with the scan rate (Fig. 3b). This indicates that the redox response corresponds to surface-confined species, maybe due to gold oxide formation and stripping.

In summary, surfactant-encapsulated POMs can self-assemble into ordered porous honeycomb films at an air/water interface. Honeycomb films of the $(DODMA)_{10}\{Mn_2Bi_2W_{20}\}$ complex were successfully used as good templates to directionally

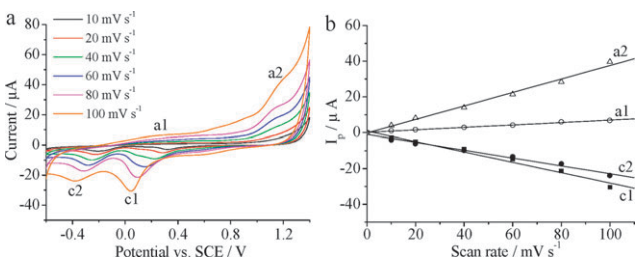

Fig. 3 (a) Cyclic voltammograms of an Au-filled honeycomb film of $(DODMA)_{10}\{Mn_2Bi_2W_{20}\}$, which was measured in a 0.1 M KNO_3 aqueous solution at different scan rates at room temperature. (b) Oxidation (a1, a2) and reduction (c1, c2) peak currents (I_p) as a function of the scan rate.

electrodeposit Au nanoparticles into their macropores, producing a hierarchical structure. Finally, we have realized that the functionalization of honeycomb films of surfactant-encapsulated POMs presents rich electrochemical properties, in our example importantly showing a strong SERS effect with R6G molecules. This suggests potential applications in devices and detectors of organic molecules.

Experimental

An $\{Mn_2Bi_2W_{20}\}$ aqueous solution was mixed with DODMACl in a molar ratio of 1 : 10. After vigorous stirring, the formed hydrophobic surfactant-encapsulated polyoxometalate (HSEP), $(DODMA)_{10}\{Mn_2Bi_2W_{20}\}$, was washed with triply-distilled water and dried. A 1.7 mg mL^{-1} chloroform solution of $(DODMA)_{10}\{Mn_2Bi_2W_{20}\}$ was cast onto an air/water interface using a microinjector at room temperature. After complete evaporation, the thin opaque solid films remained on the water surface. By carefully dipping the analytical substrates under the films and then pulling them out of the water, the films were directly transferred onto the conductive side of the ITO-coated glass. They were then dried by pure nitrogen. The bare region of the film-coated ITO-glass was next carefully covered with nail polish. Finally, the above-prepared ITO-coated glass was used as a working electrode (WE). The electrodeposition was carried out on a CHI600B electrochemical station with a three-electrode system. A Pt plate, which was cleaned by immersing it in dilute nitric acid (v : v = 1 : 1) for 5 min, was used as the counter electrode (CE). A saturated calomel electrode (SCE) was used as the reference electrode (RE). Cyclic voltammetry (CV) was undertaken in a 0.5 mM $HAuCl_4$ and 0.1 M KNO_3 aqueous solution (pH = 6.14) at room temperature. During the electrodeposition, the potential was varied between −0.6 and 0.4 V, the scan rate was 20 mV s^{-1}, and the scan time was 800 s. After the electrodeposition, the film was a little golden-colored. It was then washed before SEM observations. In addition, by the same method, using the bare ITO-coated glass as the working electrode, the electrodeposition of Au nanoparticles directly onto bare ITO-coated glass without the honeycomb film template was also performed. In order to avoid the decomposition of $HAuCl_4$ by light, the electrolytic cell was covered during the electrodeposition. All of the ITO-coated glass was cleaned before use by ultrasonication in acetone, ethanol and distilled water for 30 min, respectively.

The authors are thankful for the financial support of the NSFC (grant no. 20625307) and the National Basic Research Program of China (973 program, 2009CB930103).

Notes and references

1 G. Widawski, M. Rawiso and B. François, *Nature*, 1994, **369**, 387.
2 D. Fan, X. Jia, P. Tang, J. Hao and T. Liu, *Angew. Chem., Int. Ed.*, 2007, **46**, 3342.
3 P. Tang and J. Hao, *J. Colloid Interface Sci.*, 2009, **333**, 1.
4 D. G. Kurth, P. Lehmann, D. Volkmer, H. Cölfen, M. J. Koop, A. Müller and A. Du Chesne, *Chem.–Eur. J.*, 2000, **6**, 385.
5 S. Liu, D. G. Kurth, B. Bredenkötter and D. Volkmer, *J. Am. Chem. Soc.*, 2002, **124**, 12279.
6 W. Bu, H. Li, H. Sun, S. Yin and L. Wu, *J. Am. Chem. Soc.*, 2005, **127**, 8016.

7 H. Sun, H. Li, W. Bu, M. Xu and L. Wu, *J. Phys. Chem. B*, 2006, **110**, 24847.
8 M. Bösing, A. Nöh, I. Loose and B. Krebs, *J. Am. Chem. Soc.*, 1998, **120**, 7252.
9 T. S. Olson, P. Atanassov and D. A. Brevnov, *J. Phys. Chem. B*, 2005, **109**, 1243.
10 G. Sauer, G. Brehm, S. Schneider, K. Nielsch, R. B. Wehrspohn, J. Choi, H. Hofmeister and U. Gösele, *J. Appl. Phys.*, 2002, **91**, 3243.
11 C. Fang, E. Foca, L. Sirbu, J. Carstensen, H. Föll and I. M. Tiginyanu, *Phys. Status Solidi A*, 2007, **204**, 1388.
12 G. Duan, W. Cai, Y. Luo, Y. Li and Y. Lei, *Appl. Phys. Lett.*, 2006, **89**, 181918.
13 B. Wolfrum, Y. Mourzina, D. Mayer, D. Schwaab and A. Offenhäusser, *Small*, 2006, **2**, 1256.
14 Y. Guari, C. Thieuleux, A. Mehdi, C. Reyé, R. J. P. Corriu, S. Gomez-Gallardo, K. Philippot, B. Chaudret and R. Dutartre, *Chem. Commun.*, 2001, 1374.
15 X. Y. Zhang, L. D. Zhang, Y. Lei, L. X. Zhao and Y. Q. Mao, *J. Mater. Chem.*, 2001, **11**, 1732.
16 J. S. Dunning, D. N. Bennion and J. Newman, *J. Electrochem. Soc.*, 1971, **118**, 1251.
17 Z. H. Lin and H. T. Chang, *Langmuir*, 2008, **24**, 365.
18 J. A. Dieringer, K. L. Wustholz, D. J. Masiello, J. P. Camden, S. L. Kleinman, G. C. Schatz and R. P. Van Duyne, *J. Am. Chem. Soc.*, 2009, **131**, 849.
19 R. Gupta and W. A. Weimer, *Chem. Phys. Lett.*, 2003, **374**, 302.
20 P. Hildebrandt and M. Stockburger, *J. Phys. Chem.*, 1984, **88**, 5935.

